Numerical Simulation of a MW-Class Self Field Magnetoplasmadynamic Thruster using the MACH 2 Code

IEPC-2005-206

Presented at the 29th International Electric Propulsion Conference, Princeton University, October 31 – November 4, 2005

Brian L. England* and Pavlos G. Mikellides.†
Arizona State University, Tempe, AZ, 85283, United States of America

Abstract: The magnetohydrodynamics computer code, MACH2 is employed to model and offer further insights into the operation of a GW-level plasma source that utilized magnetoplasmadynamic, (MPD) acceleration for gas energy deposition. The facility – which operated about a year ago by using a 1.8MJ capacitor bank to produce a current pulse of the order of 1.8ms – produced mapping of the source's Current-Voltage characteristics for varying mass-flow rates. The current theoretical approach aims to validate the model at these power levels and extend performance characteristics beyond the limited experimental data. In addition, the modeling allows examination of the device as a very-high power MPD thruster by predicting thrust values for power levels up to 180MW. Accurate modeling required an upgrade of the code's circuit routines to properly capture the Pulse-Forming-Network (PFN) current waveform which also serves as the primary variable for validation. Comparisons to experimentally deduced current waveforms were in good agreement for all power levels. The simulations also produced values for the plasma voltage which were compared to the measured voltage across the electrodes. Trend agreement is encouraging while the magnitude of the discrepancy is approximately constant and interpreted as a representation of electrode fall voltage. Thrust computations have also been performed to show expected electromagnetic acceleration trends at the high power levels.

Nomenclature

r_{c1}	=	Inner Cathode Radius	r_{c2}	=	Outer Cathode Radius
r_a	=	Anode Radius	l_{c1}	=	Axial Length of Cathode Center Shaft
l_{c2}	=	Axial Length of Cathode Discharge Disk	l_a	=	Axial Length of Anode
l_e	=	Radial Length of the Exit Plane	l_t	=	Axial Length of Computational Grid
C_L	=	Center Line of the Axis of Rotation	P_0	=	Inlet Helium Pressure
R	=	Specific Gas Constant for Helium	T_0	=	Inlet Helium Temperature
ρ_0	=	Inlet Helium Density	γ	=	Ratio of Specific Heats for Helium
ζ	=	Level of Ionization	M	=	Molecular Mass of Helium
$\dot{m}$	=	Inlet Mass Flow Rate of Helium	A_i	=	Inlet Area
b	=	Geometric/Electromagnetic Thrust Constant	V	=	Plasma Voltage
J	=	Plasma Current	U_a	=	Alfven Critical Speed
Q	=	Ionization Energy of Helium	T	=	MPD Thrust
δ	=	Electromagnetic Thrust Constant	P_E	=	Electric Power
P_T	=	Thrust Power	η	=	Thrust Efficiency

* Undergraduate Honors Student, Mechanical and Aerospace Engineering Department, Brian.L.England@asu.edu.
†Assistant Professor, Mechanical and Aerospace Engineering Department, Pavlos.Mikellides@asu.edu.

I. Introduction

One of the fundamental processes in fusion propulsion concepts that lacks adequate understanding is the expansion of fusion-grade plasma through a converging-diverging magnetic field. The current effort aims to develop theoretical models to aid in the design process and understanding of such thrusters. The inability to operate a fusion facility capable of producing the power requirements for adequate duration, leads to alternative methods in designing, building and operating a facility capable of emulating fusion-grade plasma. These facilities are designed to analyze the plasma's behavior including accelerating mechanisms, levels of ionization, power requirements, and efficiency.

One such facility was constructed and operated at the Ohio State University. The necessary power levels were provided by a 1.8MJ capacitor bank configured in a Pulse Forming Network (PFN) capable discharging within a 1.8ms pulse,[1] thus producing power levels on the order of 1GW. The geometry and design of the plasma source adhered to electromagnetic energy deposition via magnetoplasmadynamic, (MPD) thruster acceleration. Through the use of this facility, multiple experiments at mass flow rates ranging from 2g/s to 30 g/s of helium propellant were conducted. The regimes that were analyzed in the research conducted reached 300MW of power and 300kA of current. The experimental data mainly characterized the Plasma Voltage–Current discharge relationship which is depicted in Fig. 1.[2]

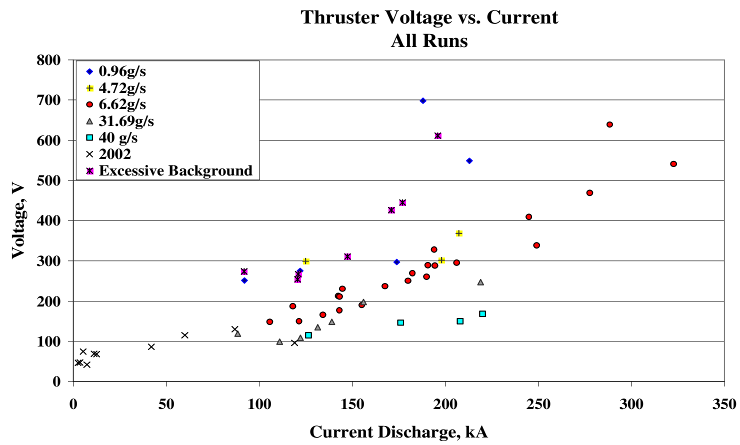

Figure 1. Voltage Current Relationship for Experimental Tests at Various Mass Flow Rates.

The goal of this research effort is to further validate the MACH 2 code by predicting thruster performance characteristics and comparing it to experimental data. Through the use of the code, additional insights into the plasma behavior are obtained and characterize the relevant physical processes.

II. MACH 2 Modeling

The MACH 2 code is a time-dependent, two-dimensional axisymmetric, single-fluid, multi-temperature, non-ideal radiation, magneto-hydrodynamics (MHD) code which has previously been used to model various laboratory experiments.[3]

A. Geometry

The computational grid defined within MACH2 consists of 12 individual blocks. This initial grid serves as a starting point for MACH 2's iterative solution of the mesh generation equations. Figure 3 shows the setup of the computational grid. The grid itself was modeled directly from the dimensions of the experimental Plasma Source which can be seen in Fig. 2.[4,5] This configuration was chosen because it facilitated the discharge across the smaller outer gap between the electrodes.

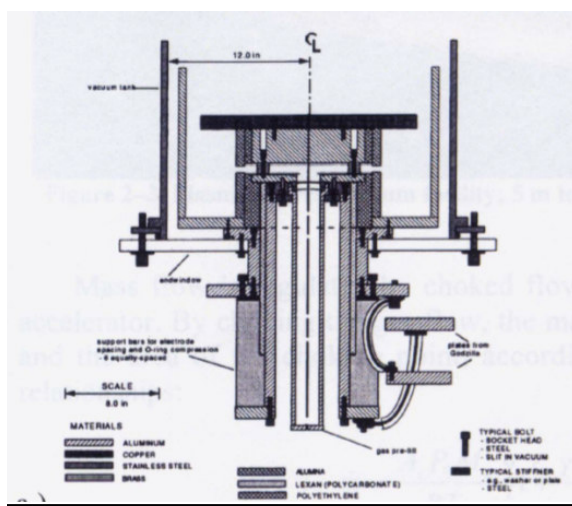

Figure 2. Schematic of the Plasma Source used in the experiments.

The experimental accelerator consists of an inner cathode radius, r_{c1}, of 5.6", an outer cathode radius, r_{c2}, of 9", and a anode radius, r_a, of 10". In addition, the axial lengths of the cathode core, l_{c1}, the entire cathode, l_{c2}, and the anode, l_a, were 8", 9.25", and 13" respectively. The radial length of the computational mesh exit plane, l_e, and the axial length of the computational test section, l_t, are 10.75" and 19.5" respectively. In the figure, C_L denotes the Center Line for the axisymetric calculations.

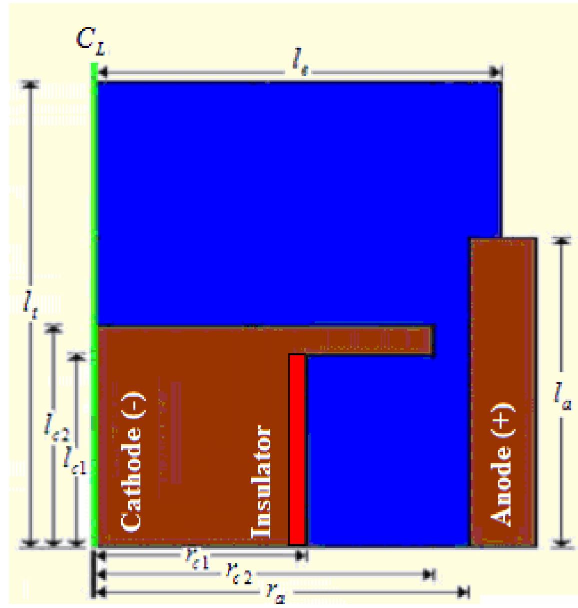

Figure 3. Thruster Geometric Configuration.

B. Boundary, Initial Conditions and PFN circuit model

The source for the experiment was incased within a vacuum tube which was initially evacuated to a pressure of 10^{-5} Torr ($1.333\text{x}10^{-3}$ Pa).[4] The initial condition inputs for MACH 2 require temperature and density values. In order to simulate the experimental pressure conditions within MACH 2, initial conditions for temperature and density were imposed upon all blocks within the computational grid. The initial temperature and densities of the computational grid were set at 0.02585 eV (300K) and $5\text{x}10^{-7}$ kg/m^3 which correspond to a pressure of $0.43\text{x}10^{-3}$ Pa. This pressure is lower than that of the experimental vacuum facility, but the difference is negligible in comparison to the densities under study during operation of the thruster. In addition, the velocity of the fluid initially in the vacuum chamber for each block was set to zero. The moderately high density, very high speed plasma implies high viscous Reynolds numbers, so free slip boundary conditions were imposed at the solid surfaces.

The discharge used in the experiment was provided by the GW-level LC-ladder capacitor bank. The bank comprises a series of 2100 capacitors and inductors in parallel. Each capacitor is rated at 43 microfarads and each inductor is rated at 2.2 micro henrys. This configuration allows the 1.6MJ stored energy to be discharged in approximately 1.63 milliseconds with a maximum current of 333 kA.[1,2] In order to properly simulate the current waverform within MACH 2, a new pulse-forming-network (PFN) circuit solver was developed and implemented. This optional code solves the following system of ordinary differential equations

$$\left[L_{p1}+L_1+L_{ext}\right]\dot{I}_1(t)-L_{p1}\dot{I}_2(t)+\left[R_{p1}+R_1+R_{ext}\right]I_1(t)-R_{p1}I_2(t)=V_1^c(t)-V_{dl}(t)$$

$$\bullet$$
$$\bullet$$

$$L_{p_{i-1}}\dot{I}_{i-1}(t)+\left[L_{p_{i-1}}+L_{p_i}+L_i\right]\dot{I}_i(t)-L_{p_i}\dot{I}_{i+1}(t)-R_{p_{i-1}}I_{i-1}(t)+\left[R_{p_{i-1}}+R_{p_i}+R_i\right]I_i(t)-R_{p_i}I_{i+1}(t)=V_i^c(t)-V_{i-1}^c(t)$$

$$\bullet$$
$$\bullet$$

$$\left[L_{p_{N-1}}+L_{p_N}+L_N\right]\dot{I}_N(t)-L_{p_{N-1}}\dot{I}_{N-1}(t)+\left[R_{p_{N-1}}+R_{p_N}+R_N\right]I_N(t)-R_{p_{N-1}}I_{N-1}(t)=V_N^c(t)-V_{N-1}^c(t)$$

where L_i and R_i are each section's inductance and resistance, respectively, L_{pi} and R_{pi} are parasitic inductance and resistance associated with capacitor, C_i, respectively, $V_i^c(t)$ are the capacitor voltages, and V_{dl} is the voltage drop across the current boundary of the MACH2 computational region; $V_{dl}=\int E\bullet dl_{circuitboundary}$. A diagram of the multiple section circuit is displayed in Figure 4, (For simplicity, the parasitic inductances and resistances are not shown.);

The solver utilizes a 4th order Runge-Kutta integration method and returns the circuit current, I_1, to the current boundary condition for MACH2. The PFN circuit is subject to the same restrictions imposed by the other circuit solvers in MACH2, and it is also controlled via the namelist $current.

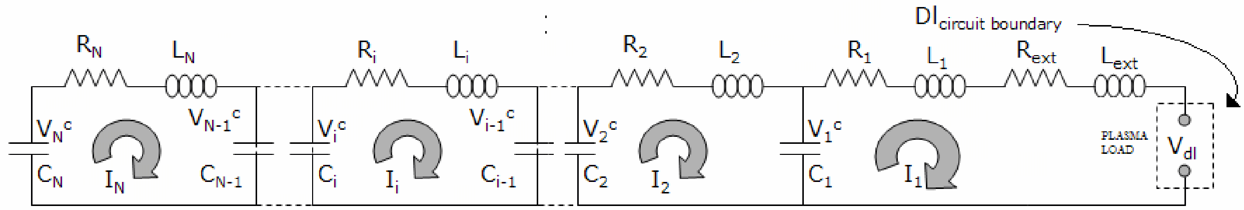

Figure 4. Schematic diagram of the PFN circuitry connected to the MACH computational domain.

C. Mass Injection System

The gas used in the experimental tests was helium. This fuel was chosen for its future applicability to High Power MPD thrusters that may be used in interplanetary missions in which the byproduct of the Fusion powered craft will be helium.[1] In the experiment, Helium was fed through the plenum, entering the discharge chamber at sonic speeds.[2] The temperature of the propellant entering the discharge chamber was 300K which prescribes the necessary inlet boundary density value,

$$\rho_0 = \frac{\dot{m}}{A_i\sqrt{\gamma T_0 R}}, \tag{1}$$

where $\dot{m}$, is 12.8 g/s which is the mass flow rate under investigation for the experimental runs, γ is the ratio of specific heat for helium which is 5/3, T_0 is the initial temperature of the helium which is 300k, R is the specific gas constant, and A_i is the inlet area which for this geometry is 0.1816 m^2. Using these values, the density of the helium propellant, ρ, at the point of entering the discharge chamber is 6.9e^{-5}kg/m^3. This value was implemented into the MACH 2 code.

D. Simulation Validation

Thruster modeling addressed operation at 12.8g/s varying the power level in accordance to the experimental range. The available variables for comparisons were the current waveform and thruster voltage the former of which was modeled by the PFN circuitry through inputs of the experimental matching resistance. Two such representative comparisons are shown in Fig. 5-8 for the 324 kA and 183kA quasi-steady current settings. As illustrated, the

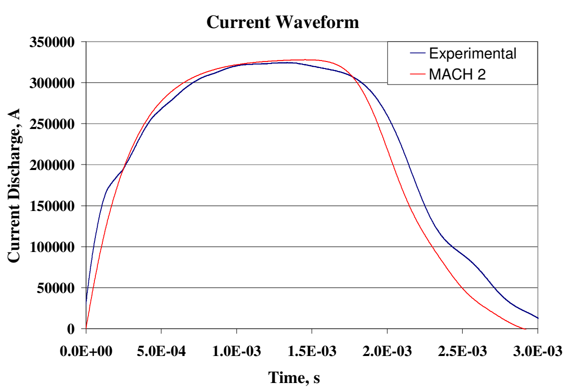

Figure 5. Current Waveform Comparison between MACH 2 and Experimental Data for the 324 kA Discharge.

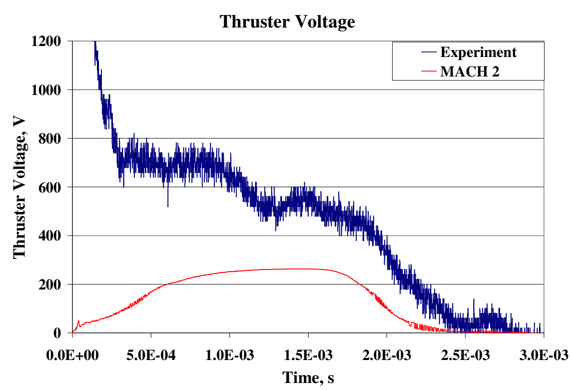

Figure 6. Voltage Comparison between MACH 2 and Experimental Data for the 324 kA discharge.

predicted current waveform's rise time as well as quasi steady state behavior is adequately captured. In addition, while the measured plasma voltage does not display perfectly quasi steady state behavior, appropriate averaging deduces effective quasi-steady state values of approximately 500V and 310V, respectively. The discrepancy between the voltage magnitude and the experimental results is accounted for by power deposition to the electrodes in the form of fall voltages. MACH 2 does not currently account for such fall voltage calculation. It is encouraging, however, to note that for both of these cases the voltage difference is constant. The quasi-steady state plasma voltage-current characteristics for all cases are depicted by Fig. 9. In addition to the normal plasma voltage – current

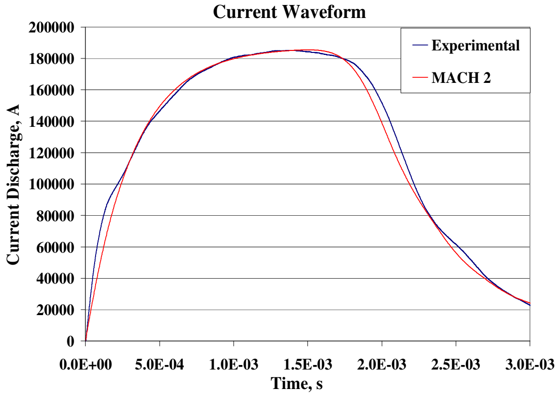

Figure 7. Current Waveform Comparison between MACH 2 and Experimental Data for the 128 kA Discharge.

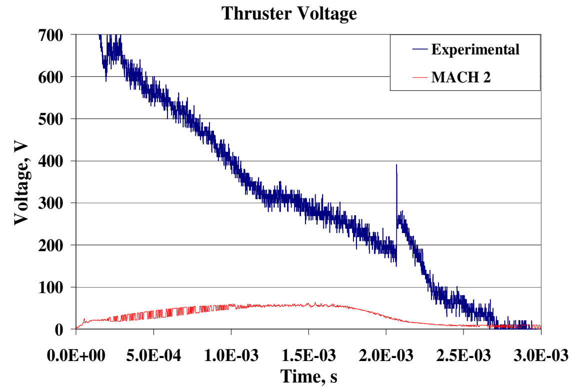

Figure 8. Voltage Comparison between MACH 2 and Experimental Data for the 128 kA discharge.

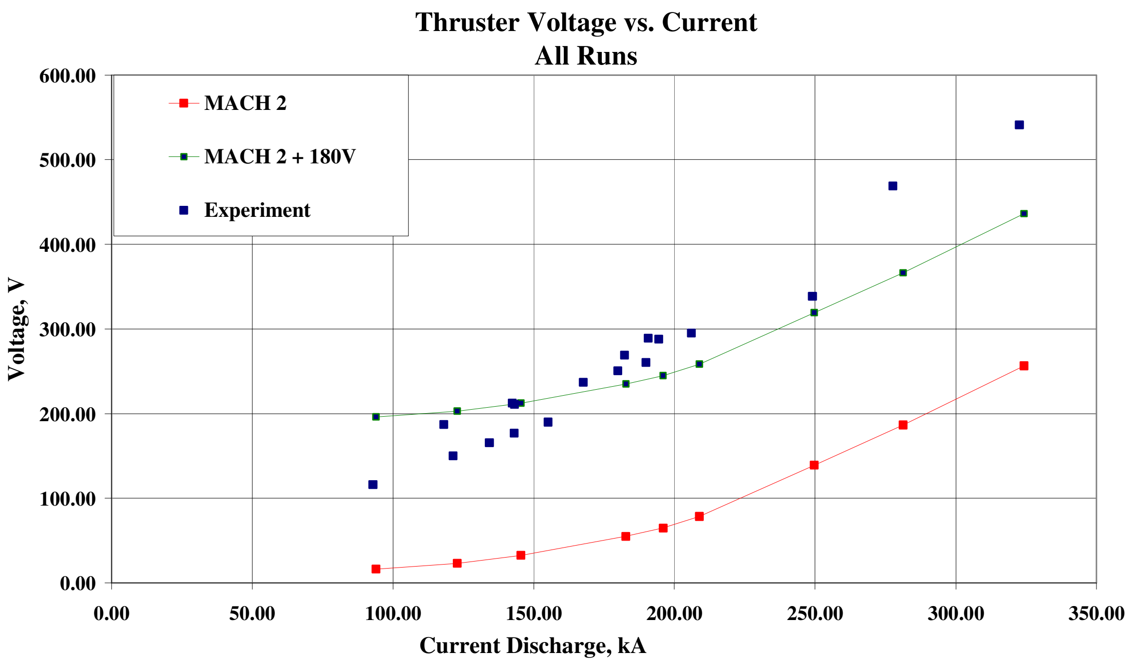

Figure 9. Comparison between Experimental and Simulated Thruster Voltage - Current Relationship.

discharge trend, an additional trend line was plotted against it in which all the values were shifted 180V in order to account for electrode power deposition, i.e. fall voltages.

It can be conjectured that for predominantly electromagnetic acceleration, i.e. high magnetic Reynolds number, the voltage drop across the plasma scales with the current through a cubic relationship,[6,7]

$$V = \frac{b^2 J^3}{2\dot{m}}. \tag{2}$$

The predicted voltage in Fig. 9 depicts such variation for lower power levels as expected. However, it has also been noted in many experiments that such a trend is no longer followed for gas velocities, U , exceeding the so-called Alfven Critical Speed, U_a , rather a linear dependence emerges which can be qualitatively extracted from limiting velocity arguments as follows:[7]

$$V = \frac{bU_a J}{2}, \tag{3}$$

For helium propellant, the Alfven critical speed can be determined by

$$U_a = \sqrt{\frac{2Q}{M}}, \tag{4}$$

where, Q and M are the first ionization energy and the molecular mass of the propellant respectively. By equating the two Voltage expressions a corresponding Alfven Critical current can be determined. For this thruster using helium propellant, the Alfven Critical speed and current were determined to be approximately, 34.4 km/s and 204.5 kA respectively. The transition from the cubic to linear relationship is evident for both experimental and calculated plasma voltage trends. The computation of such transition at critical current by MACH2 is somewhat unexpected since the phenomenon has been traditionally attributed to a combination of increased electrode erosion – the linear relationship identified by Eq. 3, inherently prescribes an increase in mass flow rate so long as thrust is attributed to electromagnetic acceleration – and voltage fluctuations due to instabilities and sputtering. None of the above physical phenomena is modeled by MACH2 which conserves mass by definition and can not capture azimuthal current variation due to its axisymmetric nature. Consequently, the calculation of such transition at critical current by MACH2 implies that the inherent mechanisms are included in the set of MHD equations in conjunction to the thermodynamic model for the equation of state. In addition, MACH2 had previously calculated the rapid ionization rate associated with the Alfven limitation within other electromagnetic devices.[3]

E. Performance Predictions

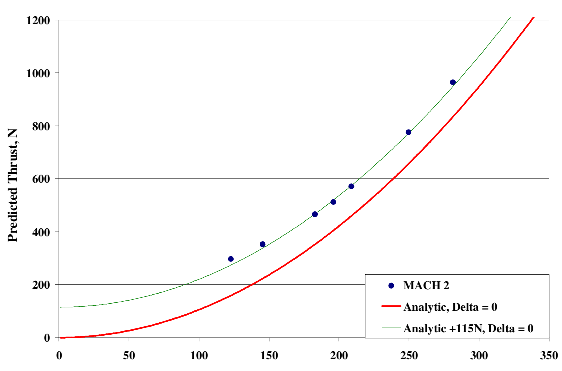

Figure 10. Comparison of Predicted Thrust of MACH 2 vs the Analytic Electromagnetic Thrust Expression.

The encouraging comparisons to experimental data allow extension of the computations to characterize thruster performance. Thrust calculations, depicted in Fig. 10, are compared to the conventional analytic model governing the thrust contribution due to electromagnetic acceleration,

$$T = bJ^2, \tag{5}$$

where the constant b is defined by the thruster geometry and current distribution as,

$$b = \frac{\mu_0}{4\pi}\left[\ln\frac{r_a}{r_c} + \delta\right], \tag{6}$$

where μ_0 is the permeability of free-space, δ is a constant that depends on the current distribution over the cathode, and r_a and r_c are the radius of the anode and cathode respectively.[4,6] The comparisons of Fig. 10 utilize δ =0 based on the computed current distribution. It is apparent that the computed thrust for current levels above 125kA conforms to the expected quadratic relationship however it is offset by an approximately constant factor of about

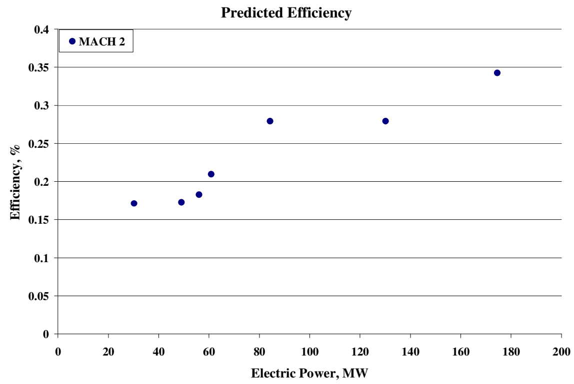

Figure 12. Predicted Efficiency of MPD Thruster for Various Current Discharge Magnitudes.

115N. This additional contribution can be attributed to enthalpy conversion due to gas expansion; however its seemingly current-independent value is somewhat unexpected.

Thrust calculation generated by the MPD thruster consequently allows prediction of the theoretical efficiency as a function of input power and/or current level. To accomplish this, the electrical and Thrust power were calculated. The thrust power was determined via the standard expression,

$$P_T = \frac{F^2}{2\dot{m}}. \tag{7}$$

The input power calculation was then determined using the expression for electric power,

$$P_E = JV\ . \tag{8}$$

The value of the voltage used in this calculation was the voltage obtained from experimental results to account for the total thruster operating power. Using these values, the predicted thruster's efficiency was calculated as,

$$\eta = \frac{P_T}{P_E}. \tag{9}$$

The calculated efficiency values are shown in Fig. 12 as a function of thruster power and are typical of such thruster operation ranging from 0.17 to 0.35. It is also heartening to note the typical increase in efficiency with increasing power levels which is also typical of such MPD acceleration. Both thruster and efficiency calculations establish the highest power MPD thruster ever operated with power level as high as 180MW producing thrust values of the order of 1000N.

F. Plasma Properties

In order to further characterize thruster operation and conditions it is insightful to investigate the quasi-steady two-dimensional distributions of the plasma properties. Utilizing MACH2's interfacing capability with the extensive graphing program, tecplot, the pertinent gas properties could be plotted for the entire computation mesh to show each of their respective distributions. Each case under investigation was a specific power range of interest for a mass flow rate of 12.8g/s for helium propellant. The power ranges that were analyzed were: 30MW, 61MW, and 180 MW, which each corresponded to a maximum current discharge of 145kA, 208kA, and 324kA respectively. These discharge currents were chosen to be representative of the current discharge at low, medium, and high power levels. It also has the added benefit of depicting the current discharges less than the Alfven Critical Current, approximately equal to Alfven Critical Current, and much greater than that of the Alfven Critical Current.

Figures 13-17 show the pertinent 2-dimensional distributions for the high power case and Fig. 18-27 show the 2-dimensional distributions for the low and medium power cases. The current distribution identifies the consequence of the electrode design geometry diverting the plasma towards the centerline. MACH2 prescribes plasma reaching maximum speeds exceeding 100km/s, fully-doubly ionized helium of maximum temperature values of the order of 90ev. Such temperature distribution is of paramount importance in an attempt to emulate the conditions expected for fusion applications to magnetic nozzle acceleration and should be of the order of 100ev. The equivalent total temperature values for each case were calculated using the following expression,

$$(1+\zeta)C_P T_0 = \frac{\int (1+\zeta)C_P T_i \rho U dA}{\dot{m}} + \frac{U^2}{2} \tag{10}$$

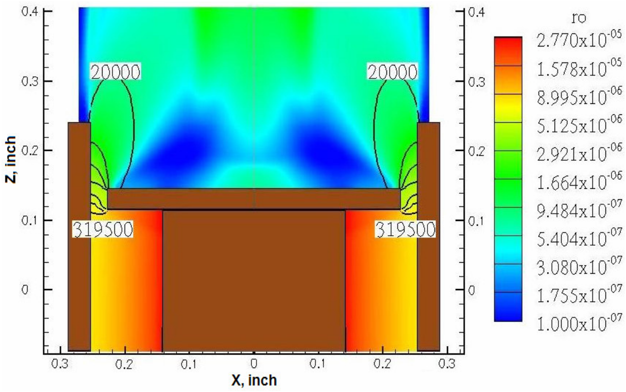

Figure 13. Plasma density and current distribution for the 322kA discharge.

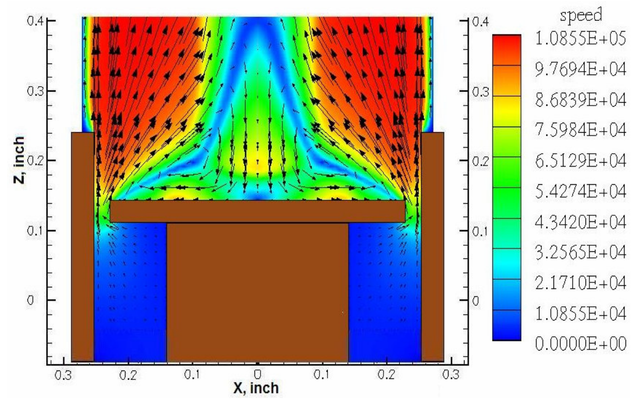

Figure 14. Velocity vectors and speed distribution for the 322kA discharge.

where ζ is the ionization level.

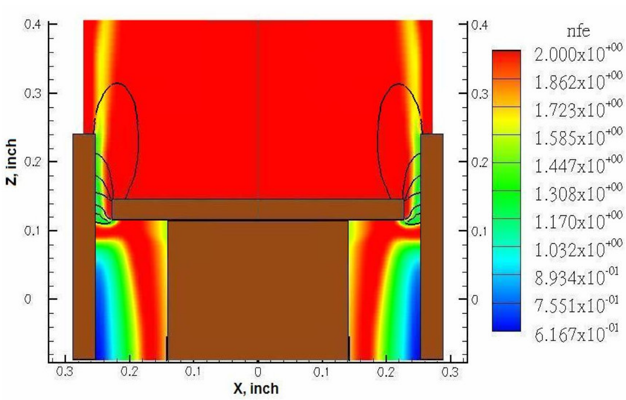

Figure 15. Propellant ionization level (average charge) for the 322kA discharge.

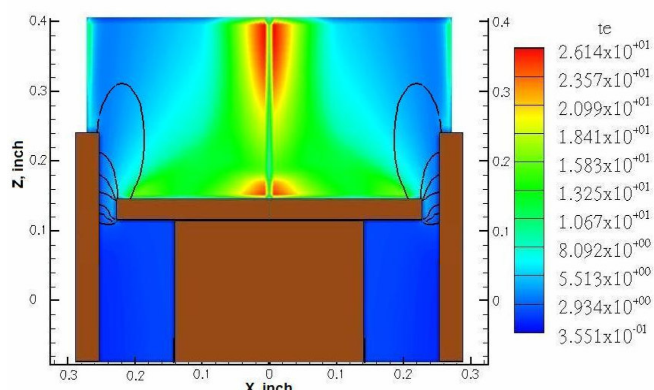

Figure 16. Electron temperature distribution for the 322kA discharge.

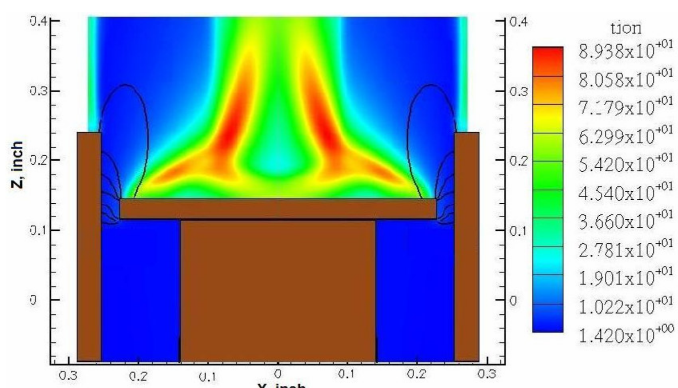

Figure 17. Ion temperature distribution for the 322kA discharge.

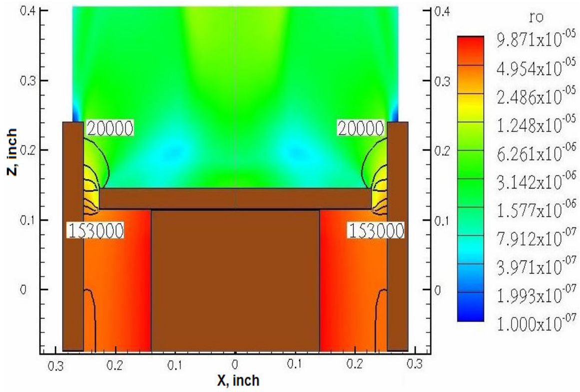

Figure 18. Plasma density distribution for the 145 kA discharge.

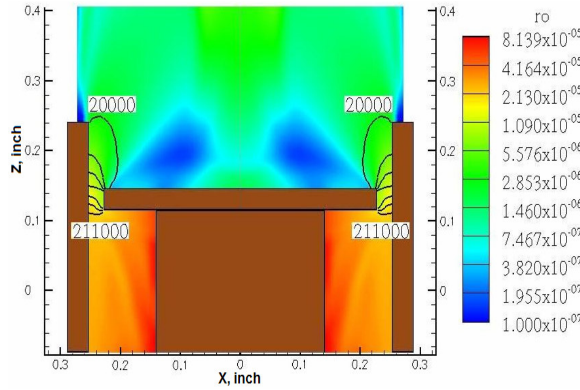

Figure 19. Plasma density distributions for the 209 kA discharge.

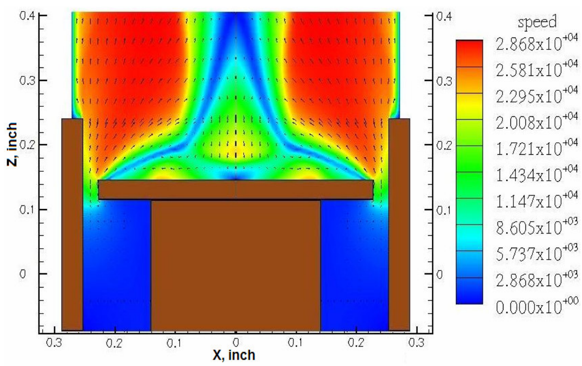

Figure 20. Velocity profile for the 145 kA discharge.

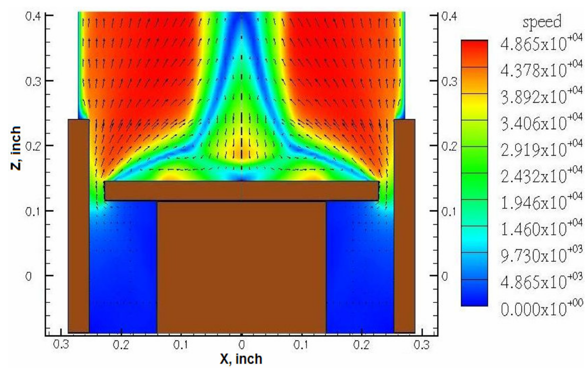

Figure 21. Velocity profile for the 209 kA discharge.

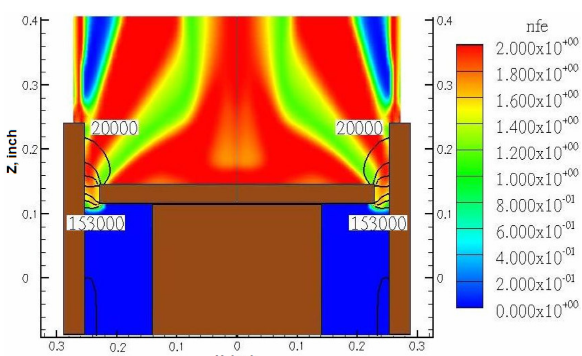

Figure 22. Propellant ionization levels for the 145 kA discharge.

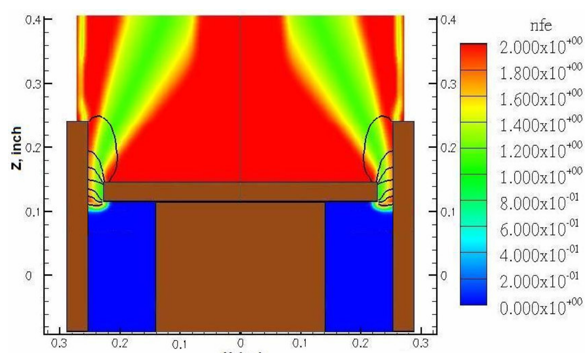

Figure 23. Propellant ionization levels for the 209 kA discharge.

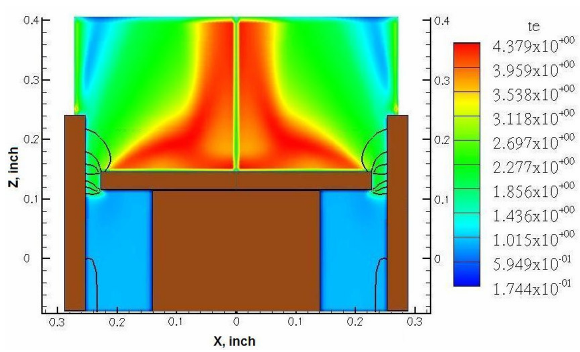

Figure 24. Electron temperature distrubtion for the 145 kA discharge.

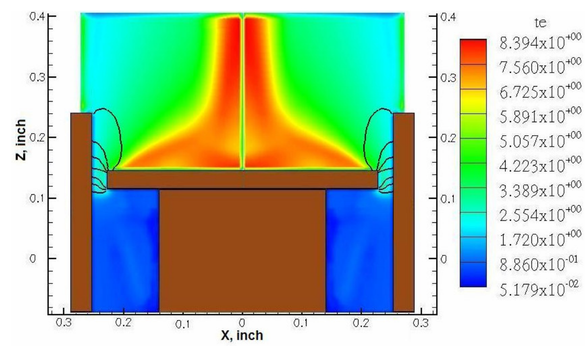

Figure 25. Electron temperature distribution for the 209 kA discharge.

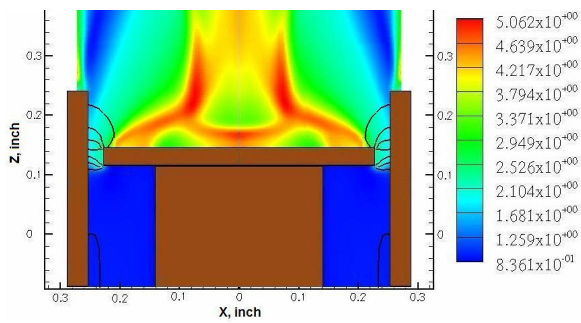

Figure 26. Ion temperature distrubtion for the 145 kA discharge.

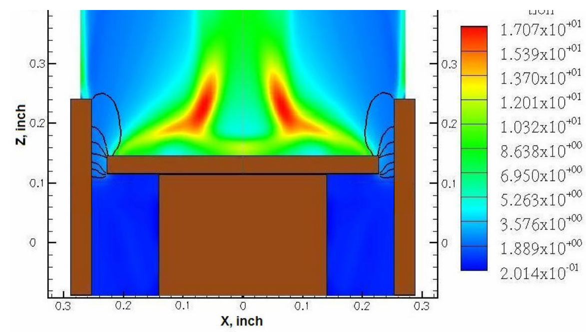

Figure 27. Ion temperature distribution for the 209 kA discharge.

The appropriate variable profiles were numerically integrated along the exit plane of the thruster. The predicted stagnation temperatures for the 145kA, 208kA, and 324kA current discharges were 1.6eV, 4.6eV, and 21eV, respectively. Even though for this particular mass-flow rate operation, 12.8g/s, the projected stagnation temperature values do not reach the fusion rocket required regimes they still reflect plasma that can be utilized to study the pertinent processes. Furthermore, we note that the source has successfully operated at mass-flow rates, 2g/s-30g/s which will most certainly provide stagnation temperatures exceeding 100eV. Specifically, we note that such stagnate flow will produce temperature values that scale with the square of the thrust, and inversely proportional to the square of the mass-flow rate,

$$\overline{T}_o \sim \frac{(\gamma-1)F^2}{2(1+\zeta)\gamma R\dot{m}^2} \sim \frac{(\gamma-1)b^2 J^4}{2(1+\zeta)\gamma R\dot{m}^2}. \tag{11}$$

This projects stagnation temperature values exceeding 250eV when the source is operated at 3.5g/s.

III. Conclusions

A very-high power (180MW) magnetoplasmadynamic, (MPD) plasma source/thruster was modeled using the magnetohydrodynamic, (MHD) code, MACH2 at a helium mass-flow rate of 12.8g/s. The code utilized a new Pulse-Forming-Network, (PFN), circuit model to emulate the current pulse. Comparisons of the predicted current waveform profiles and Voltage-Current characteristics to the experimental data were in very good agreement lending confidence to the code's predictive capabilities as well as to the integrity of the experimental process. Both theory and experiment display the expected voltage transition from the typical cubic relationship to a linear dependence as a function of current for thruster velocities exceeding Alfven critical speed. Computed thrust values conform to the expected electromagnetic quadratic dependence as a function of current with an additional constant thrust contribution due to enthalpy conversion. Based on these values, the thruster operated at efficiencies ranging from 0.17 at the lowest power level to 0.35 when operated at 180MW and quasi-steady current value of 324kA. Gas properties entail fully-doubly ionized helium exceeding particle temperature of 90eV and reaching speeds in excess of 100km/s. Projected stagnation temperature values at 12.8g/s operation exceed 20eV which implies that the source produced the necessary conditions to establish stagnation temperatures of the order of 250eV when it operated within 3g/s-4g/s.

IV. References

[1]Turchi, P.J., "Design of a Gigawatt-Level, Quasi-Steady Flow Facility for Advanced Space Exploration Research." AIAA-1991-3613, AIAA/NASA/OAI Conference on Advanced SEI Technologies, Cleveland, Ohio, Sept. 1991.

[2]Gilland, James H., Mikellides, I., Mikellides, P., Gregorek, G., and Marriott, D., "Magnetic-Nozzle Studies for Fusion Propulsion Applications: Gigawatt Plasma Source Operation and Magnetic Nozzle Analysis." NASA Glenn Cooperative Agreement, NAG3-2601.

[3]Peterkin, R.E., Jr., and Frese, M.H., "MACH: A Reference Manual – First Edition," Air Force Research Laboratory: Phillips Research Site, 1998.

[4]Marriott, D., *et al.*, "Performance of a MPD Plasma Source and Magnetic Nozzle for Fusion Propulsion." AIAA-2002-3934, 38th Joint Propulsion Conference and Exhibit, Indianapolis, Indiana, July 2002.

[5]Mikellides, P.G., Turchi, P.J., and Mikellides, I.G., "Design of a Fusion Propulsion System, Part 1: Gigawatt-Level Magnetoplasmadynamic Source," *Journal of Propulsion and Power,* Vol 18, No. 1, Jan. 2002.

[6]Jahn, R. G. *Physics of Electric Propulsion,* McGraw-Hill, New York, 1968, pp. 240-245.

[7]Gilland, J. H., Kelly, A. J., and Jahn, R.G., "MPD Thruster Scaling," AIAA-87-0997, 19th International Electric Propulsion Conference, Colorado Springs, CO, May, 1987.